Proteomic Science
https://www.sciltp.com/journals/psci

Article

Distinct Skeletal Muscle Proteomic Profiles after Single and Repeated Intermittent Clenbuterol Administration in Mice

Keisuke Hitachi [1,*], Hisateru Yamaguchi [2,3], Yuri Kiyofuji [1] and Kunihiro Tsuchida [1,*]

[1] Division for Therapies against Intractable Diseases, Center for Medical Science, Fujita Health University, Toyoake 470-1192, Japan
[2] Department of Management Nutrition, Aichi Gakusen University, Okazaki 444-8520, Japan
[3] Department of Biomedical Molecular Sciences, Fujita Health University School of Medicine, Toyoake 470-1192, Japan
* Correspondence: hkeisuke@fujita-hu.ac.jp (K.H.); tsuchida@fujita-hu.ac.jp (K.T.)

How To Cite: Hitachi, K.; Yamaguchi, H.; Kiyofuji, Y.; et al. Distinct Skeletal Muscle Proteomic Profiles after Single and Repeated Intermittent Clenbuterol Administration in Mice. *Proteomic Science* **2026**, *1*(1), 3.

Received: 26 July 2026
Revised: 8 October 2026
Accepted: 10 November 2026
Published: 17 November 2026

Abstract: Clenbuterol (CB), a β2-adrenergic receptor agonist, is known to increase skeletal muscle mass, but the proteomic changes associated with repeated intermittent CB administration remain poorly characterized. We compared plantaris muscle proteomes from mice receiving CB only during the final 2-week treatment period (single CB) or during three 2-week periods separated by 4-week washout intervals (repeated CB), along with untreated controls. Label-free quantitative proteomics identified 49 and 74 differentially abundant proteins in the single and repeated CB groups, respectively, relative to controls, and 32 proteins differed between the two CB-treated groups. Functional enrichment analysis of these protein sets identified terms related to lipid metabolism in the single CB group, muscle structure and intracellular protein transport in the repeated CB group, and muscle contraction and endosomal transport in the direct comparison between the CB-treated groups. The differentially abundant proteins were further classified according to their abundance patterns, including sustained, reinforced, and repeated-specific response classes. Immunoblotting showed increases in Klhl40 and Napa (sustained class) and Galectin-3 (reinforced class) in both CB-treated groups, whereas Rab18 (repeated-specific class) was significantly increased relative to controls only in the repeated CB group. Together, these findings indicate that single and repeated CB treatments were associated with overlapping but distinct skeletal muscle proteomic profiles, providing a foundation for future studies of the effects of CB administration regimens and prior exposure.

Keywords: clenbuterol; skeletal muscle; β2-adrenergic stimulation; proteomics; muscle hypertrophy; repeated exposure

1. Introduction

Skeletal muscle is a highly plastic tissue that adapts its mass and functional properties in response to physical activity, nutritional status, neural activity, endocrine stimuli, and pharmacological interventions. Among pharmacological stimuli, β2-adrenergic receptor stimulation has been widely studied because of its effects on skeletal muscle mass, metabolism, and body composition [1,2]. Clenbuterol (CB) is a β2-adrenergic receptor agonist that has been extensively used as an experimental anabolic stimulus in skeletal muscle research. Animal studies have shown that CB administration increases skeletal muscle mass and can suppress muscle loss in models of muscle atrophy [3,4]. In addition, the hypertrophic and anti-atrophic effects of CB are preserved in β1-adrenergic receptor-deficient mice but abolished in β2-adrenergic receptor-deficient mice, demonstrating that the

Copyright: © 2026 by the authors. This is an open access article under the terms and conditions of the Creative Commons Attribution (CC BY) license (https://creativecommons.org/licenses/by/4.0/).
Publisher's Note: Scilight stays neutral with regard to jurisdictional claims in published maps and institutional affiliations.

skeletal muscle effects of CB require β2-adrenergic receptors [4]. Consistent with the broader role of β2-adrenergic receptor signaling in skeletal muscle, other β2-adrenergic agonists, including formoterol and salmeterol, have also been reported to induce skeletal muscle hypertrophy in animal models [5]. More recently, chronic CB treatment has been shown to improve glucose metabolism in a skeletal muscle β2-adrenergic receptor- and Gs-dependent manner and to induce transcriptomic and metabolomic reprogramming in skeletal muscle cells [6]. Furthermore, β-arrestin 1 has been shown to be required for CB-induced skeletal muscle hypertrophy and changes in contractile properties in vivo as a downstream mechanism of β2-adrenergic receptor signaling [7].

The effects of CB are highly dependent on treatment conditions. Low-dose CB can induce skeletal muscle hypertrophy, whereas higher doses are associated with myotoxicity [8]. Chronic CB treatment has been reported to reduce β-adrenoceptor density in skeletal muscle [9]. In addition, CB decreases β2-adrenoceptor mRNA expression in fast-twitch fiber-enriched muscles, including the plantaris muscle, without altering its expression in the soleus muscle [10]. Together, these findings indicate that the effects of CB on skeletal muscle depend on treatment conditions, including dose and duration. However, the molecular consequences of repeated intermittent CB administration remain incompletely understood.

CB is also important from sports-science and social perspectives. The World Anti-Doping Agency lists CB as a prohibited anabolic agent and prohibits it at all times, both in- and out-of-competition (World Anti-Doping Code International Standard Prohibited List 2026). In addition, CB has been used illegally as a growth-promoting agent in livestock, and unintentional positive doping cases caused by contaminated meat have been reported [11,12]. Distinguishing intentional CB misuse from exposure through contaminated meat has also been examined as an important issue in sports doping [13]. In cases of CB misuse for fat loss or muscle gain, adverse events such as tachycardia, hypokalemia, electrocardiographic abnormalities, and rhabdomyolysis have been reported [14,15]. Thus, although CB has clear pharmacological effects on skeletal muscle, understanding the molecular changes caused by repeated exposure or misuse is important from both basic biological and anti-doping perspectives.

Skeletal muscle adaptation is established through molecular changes across multiple levels, including not only the accumulation and degradation of myofibrillar proteins, but also changes in fiber type, metabolic properties, extracellular matrix organization, and inflammatory and repair responses. Therefore, to understand the effects of β2-adrenergic receptor stimulation on skeletal muscle, it is important to capture global changes in protein expression profiles rather than focusing only on a single signaling pathway or representative markers of muscle hypertrophy. A previous study investigating CB-induced changes in the skeletal muscle proteome used rat plantaris muscle and showed, by histochemical analysis and 2D gel-based proteomic analysis, that low-dose, non-myotoxic CB treatment was associated with increased plantaris muscle weight, protein accretion, and preferential hypertrophy of fast oxidative glycolytic fibers [16]. In addition, a recent mass spectrometry (MS)-based proteomic analysis of human skeletal muscle reported that prolonged β2-adrenergic stimulation with terbutaline induces proteome remodeling that shares multiple features with resistance training, including changes in translational capacity-related proteins and increased abundance of kelch-like family proteins such as KLHL40 and KLHL41 [17]. However, proteomic comparisons between single and repeated intermittent CB administration remain limited, and it is unclear which protein abundance patterns are shared between these regimens and which differ.

In this study, we established a repeated intermittent CB administration model in mice by combining 2-week treatment periods with 4-week washout periods. We then performed label-free quantitative proteomic analysis of plantaris muscles from control mice, mice exposed to a single period of CB treatment, and mice exposed to repeated CB treatment. Furthermore, by integrating three pairwise group comparisons, we classified proteins according to their abundance patterns across the experimental groups. Finally, representative proteins identified by proteomic analysis were examined by immunoblotting. This approach characterized shared and distinct endpoint proteomic features associated with single and repeated intermittent CB administration.

2. Materials and Methods

2.1. Animals, Experimental Design, and Muscle Weight Measurement

All mice were maintained in a temperature-controlled animal room at 25 °C under a 12-h light/12-h dark cycle, with ad libitum access to chow and drinking water. Male C57BL/6NJ mice were obtained from the Jackson Laboratory Japan, Inc. (Yokohama, Japan) and used from 9 weeks of age.

Clenbuterol (CB; FUJIFILM Wako Pure Chemical Corporation, Osaka, Japan) was supplied through the drinking water at 20 ppm (20 μg/mL) during each 2-week administration period. CB-containing drinking water was freshly prepared and replaced weekly during each treatment period. This concentration and treatment duration were based on a previous study [18].

In the short-term treatment and recovery experiment (Supplementary Figure S1), mice received drinking water with or without CB for 2 weeks. Muscles were collected either immediately after the 2-week treatment period or after an additional 4-week period without CB. Control and CB-treated groups were included at both collection time points.

For the repeated intermittent protocol, animals were divided into control, single CB, and repeated CB groups. The schedule comprised three 2-week treatment windows separated by 4-week intervals (Figure 1A). Control mice received unsupplemented drinking water during all three windows. Single CB mice received unsupplemented drinking water during the first two windows and CB-containing water only during the final window. Repeated CB mice received CB-containing water during each of the three treatment windows. Animals were euthanized at the end of the final 2-week treatment period. Body weight was recorded immediately before tissue collection. Gastrocnemius (Gast), plantaris, and soleus muscles were excised, weighed immediately, snap-frozen in liquid nitrogen, and kept at −80 °C until use.

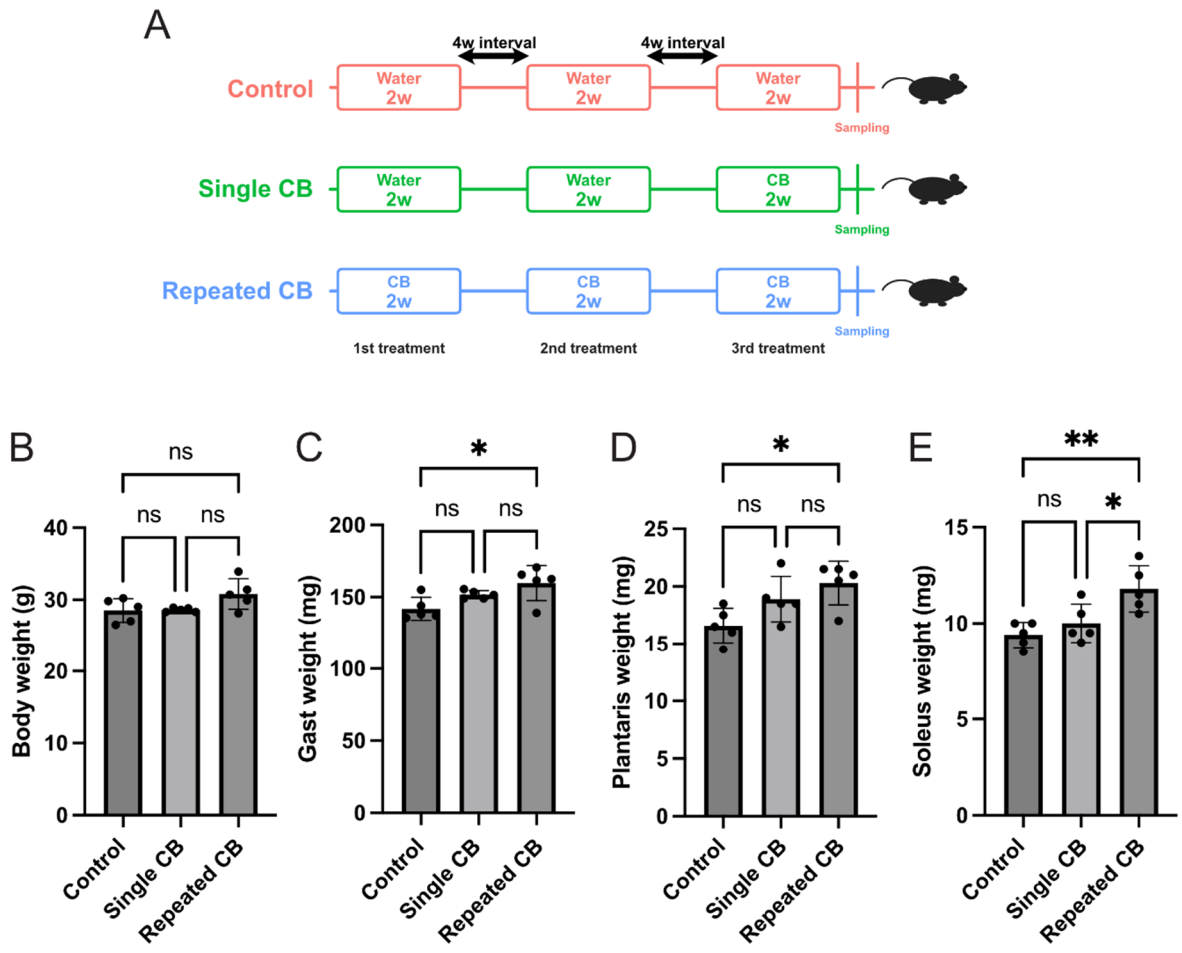


Figure 1. Repeated intermittent CB exposure produced a distinct muscle-weight response. (**A**) Experimental design of control, single CB, and repeated CB groups. The experimental timeline consisted of three 2-week treatment periods separated by 4-week intervals. Control mice received drinking water without CB during all three treatment periods. Single CB mice received drinking water without CB during the first and second treatment periods and CB-containing drinking water during the final treatment period. Repeated CB mice received CB-containing drinking water during all three treatment periods. Muscles were collected at the end of the final treatment period. (**B**–**E**) Body weight (**B**), Gast weight (**C**), plantaris weight (**D**), and soleus weight (**E**) in control, single CB, and repeated CB mice. Data are presented as mean ± s.d.; n = 5 mice per group. Data were analyzed by ordinary one-way ANOVA followed by Tukey's multiple-comparison test. ns, not significant; * $p < 0.05$; ** $p < 0.01$.

2.2. Proteomic Analysis

Plantaris muscles from four biologically independent mice per group (n = 4 per group; 12 mice in total) were processed for label-free proteomics. These mice were a subset of the five mice per group used for muscle-weight

measurements. Frozen muscles were disrupted with a Shakeman 2 homogenizer (Bio Medical Science Inc., Tokyo, Japan) in RIPA buffer consisting of 50 mM Tris-HCl (pH 7.2), 150 mM NaCl, 0.1% SDS, 1% Triton X-100, and 0.5% sodium deoxycholate, supplemented with 4 μg/mL leupeptin, 1 mM PMSF, and 1 μg/mL aprotinin, based on previously used procedures [19,20]. Protein concentration was measured with the BCA Protein Assay Kit (Takara Bio, Kusatsu, Japan). Ten micrograms of total protein from each sample was subjected to SP3-based sample preparation [21]. Samples were reduced with dithiothreitol (DTT), alkylated with iodoacetamide (IAA), and digested with Trypsin/Lys-C Mix (Promega, Madison, WI, USA) at a 1:50 enzyme-to-substrate ratio. The resulting peptides were cleaned up with GL-Tip SDB tips (GL Sciences, Tokyo, Japan) before LC-MS/MS.

Peptide separation and MS acquisition were performed using an EASY-nLC 1000 nano-liquid chromatography system coupled to an Orbitrap Fusion ETD mass spectrometer (Thermo Fisher Scientific, Waltham, MA, USA). Peptide samples were first trapped on an Acclaim PepMap 100 C18 column (3 μm, 75 μm ID × 20 mm; Thermo Fisher Scientific) and then separated on an EASY-Spray C18 analytical column (3 μm, 75 μm ID × 150 mm; Thermo Fisher Scientific). A 0–35% acetonitrile gradient in 0.1% formic acid was run at 300 nL/min. The spray voltage was 2 kV, and the ion transfer tube was maintained at 275 °C. Xcalibur software (version 4.7.69.37; Thermo Fisher Scientific) was used for data-dependent acquisition. MS1 scans were recorded over an m/z range of 375–1500 at a resolution of 120,000. The most abundant precursor ions were subjected to collision-induced dissociation in the linear ion trap with a normalized collision energy of 35%, and dynamic exclusion was set to 60 s.

MS raw files were analyzed in Proteome Discoverer version 2.4.1.15 (Thermo Fisher Scientific) using SequestHT and Mascot (version 2.6.2). Spectra were searched against the Mus musculus UniProtKB database (TaxID = 10090; version 202104), to which an additional Myh2 entry (UniProt G3UW82) was added. Cysteine carbamidomethylation was used as a fixed modification, whereas methionine oxidation and protein N-terminal acetylation were used as variable modifications. The precursor and fragment ion tolerances were 10 ppm and 0.6 Da, respectively. Trypsin digestion was searched with a maximum of two missed cleavages. Peptide-spectrum matches were filtered by target-decoy searching at a 1% false discovery rate. Label-free abundance values were obtained in Proteome Discoverer with the Precursor Ions Quantifier workflow using Minora feature detection.

For protein-detection counts, proteins with Number of Peptides ≥ 2 were retained. For principal component analysis (PCA), proteins with Number of Peptides ≥ 2 that were quantified in all 12 samples were used. Abundance values were log2-transformed, and each sample was median-normalized by shifting its median to the median across the 12 sample-specific medians. PCA was performed in R using the prcomp function with centering and without scaling.

Differential protein abundance was analyzed in Perseus v1.6.15.0 [22]. Protein abundance values were transformed to log2 scale, and each sample was median-centered to reduce sample-level intensity offsets. Missing entries were replaced using the standard Perseus imputation settings applied here: Gaussian width = 0.3 and downshift = 1.8. Pairwise differences in protein abundance were evaluated using Student's *t*-tests in Perseus. Proteins were considered differentially changed based on a nominal p value < 0.05, $|\log2 \text{ fold change}| \geq \log2(1.5)$, and Number of Peptides ≥ 2. The fold-change cutoff was used to focus on changes of appreciable magnitude, and the two-peptide requirement was applied to avoid relying on single-peptide protein identifications. No multiple-testing correction was applied to the primary differential-change criteria. The three comparisons used for this analysis were single CB versus control, repeated CB versus control, and repeated CB versus single CB. Differentially changed proteins are reported in Supplementary Table S1.

To characterize protein abundance patterns across the control, single CB, and repeated CB groups, proteins meeting the differential-abundance criteria in at least one of the three pairwise comparisons were classified into response classes. Classification was based on the comparisons in which each protein met the differential-abundance criteria, the direction of change, and the relative magnitude of the changes. The relative magnitude was calculated as the ratio of the absolute log2 fold change for repeated CB versus control to that for single CB versus control. Ratios of 0.75–1.25 (within ±25% of 1.0), >1.25, and <0.75 were used to define comparable, larger, and smaller changes, respectively. Repeated-specific proteins were defined as proteins that met the differential-change criteria in repeated CB-treated muscles compared with control muscles but did not meet these criteria in single CB-treated muscles compared with control muscles. Single-versus-repeated difference-only proteins were defined as proteins that met the differential-change criteria in the repeated CB versus single CB comparison but did not meet these criteria in either comparison with the control group. Sustained proteins were defined as proteins that met the differential-change criteria in both comparisons with the control group and changed in the same direction, with the absolute response to repeated CB ranging from 0.75-fold to 1.25-fold of the absolute response to single CB. Reinforced proteins were defined as proteins that met the differential-change criteria in both comparisons with the control group and changed in the same direction, with the absolute response to repeated CB greater than 1.25-fold of the absolute response to single CB. Single-specific/weakly attenuated proteins were defined as proteins

that met the differential-change criteria in single CB-treated muscles compared with control muscles but did not meet these criteria in repeated CB-treated muscles compared with control muscles, with the absolute response to repeated CB remaining at least 0.75-fold of the absolute response to single CB. Attenuated to baseline proteins were defined as proteins that met the differential-change criteria in single CB-treated muscles compared with control muscles but did not meet these criteria in repeated CB-treated muscles compared with control muscles, with the absolute response to repeated CB reduced to less than 0.75-fold of the absolute response to single CB. Attenuated proteins were defined as proteins that met the differential-change criteria in both comparisons with the control group and changed in the same direction, with the absolute response to repeated CB less than 0.75-fold of the absolute response to single CB. Reversed proteins were defined as proteins that met the differential-change criteria in both comparisons with the control group but changed in opposite directions. Proteins that did not match these defined patterns were assigned to an unclear-response category. Response-class assignments are provided in Supplementary Table S2.

Functional enrichment analysis was performed separately for the three pairwise comparisons using Metascape with default enrichment criteria [23]. Upregulated and downregulated proteins were analyzed together because the numbers of differentially abundant proteins were relatively small and the analysis was intended to characterize the functions represented in each complete protein set. The custom background consisted of proteins in the corresponding proteomic comparison meeting Number of Peptides ≥ 2. Enrichment results are presented as $-\log10(p)$ (Supplementary Figure S2).

Protein-count, PCA, and volcano plots were generated in R using the ggplot2 package, with ggrepel used for sample or protein labels. Response-class heatmaps were generated using the pheatmap package, and the two heatmap panels were combined using the gridExtra package. For heatmap visualization, sample-level protein abundance values were converted to row-wise z-scores. Proteins and samples were not hierarchically clustered; proteins were grouped according to their response-class assignments.

2.3. Immunoblotting

Selected proteins highlighted by the proteomic analysis were examined by immunoblotting. Plantaris muscles were extracted in the same RIPA buffer containing protease inhibitors as described above. Homogenates were centrifuged at 15,000× g for 30 min at 4 °C, and the supernatants were used as cleared lysates. Protein amounts were measured with the BCA Protein Assay Kit (Takara Bio).

Equivalent amounts of total protein were resolved by SDS-PAGE and electrotransferred to PVDF membranes. Membranes were blocked in skim milk/TBST and then reacted overnight at 4 °C with primary antibodies. The antibodies used were anti-Klhl40 (1/2000, 21836-1-AP, Proteintech, Rosemont, IL, USA), anti-Napa (1/2000, 10546-1-AP, Proteintech), anti-Galectin-3 (1/2000, AF1197, R&D Systems, Inc., Minneapolis, MN, USA), anti-Rab18 (1/2000, 11304-1-AP, Proteintech), and anti-α-tubulin (1/2000, #2144, Cell Signaling Technology, Danvers, MA, USA). Can Get Signal reagent (Toyobo, Osaka, Japan) was used for α-tubulin detection. HRP-conjugated anti-rabbit IgG (1/10000, #7074, Cell Signaling Technology) and anti-goat IgG (H + L) (1/10000, 81-1620, Thermo Fisher Scientific) served as secondary antibodies. Chemiluminescent detection was performed with ImmunoStar LD reagent (FUJIFILM Wako Pure Chemical, Osaka, Japan), and images were acquired with a cooled CCD imaging system (Light-Capture, ATTO, Tokyo, Japan). Band density was measured in Fiji ver. 2.16.0 and normalized to α-tubulin. Full-length immunoblot images are shown in Supplementary Figure S3.

3. Results

3.1. Repeated Intermittent CB Exposure Produced a Distinct Muscle-Weight Response under a Long-Term Treatment Schedule

We first examined whether the increase in muscle mass induced by a 2-week CB treatment persisted after treatment cessation. Mice were treated with or without CB for 2 weeks, and muscles were collected either immediately after this treatment period or after an additional 4-week period without CB. Control and CB-treated groups were included at both collection time points. Body weight did not differ significantly between control and CB-treated mice at either time point (Supplementary Figure S1A). At the end of the 2-week treatment period, CB significantly increased Gast and plantaris weights compared with the corresponding control groups, whereas these differences were no longer significant after the additional 4-week period without CB (Supplementary Figure S1B,C). Soleus weight did not differ significantly between the control and CB-treated groups after the 2-week treatment (Supplementary Figure S1D).

Based on this observation, we designed a repeated intermittent CB protocol to compare control, single CB, and repeated CB groups under the same long-term experimental timeline (Figure 1A). Muscles were collected at the end of the final 2-week treatment period. Body weight did not significantly differ among the three groups (Figure 1B). In contrast, repeated CB mice showed significantly increased Gast, plantaris, and soleus weights compared with control mice (Figure 1C–E). The single CB-treated group showed modest numerical increases in several muscle weights, but these did not reach statistical significance relative to controls. In addition, soleus weight was significantly higher in repeated CB mice than in single CB mice (Figure 1E).

3.2. Proteomic Profiling Revealed Different Global Patterns after Single and Repeated CB Exposure

To determine whether the different muscle-weight responses were accompanied by changes in protein abundance, we performed proteomic analysis of plantaris muscles from control, single CB, and repeated CB mice. Protein-detection depth was comparable among samples after peptide-based filtering (Figure 2A). PCA of commonly quantified proteins showed that single CB samples had a more dispersed distribution, whereas repeated CB samples formed a more compact cluster (Figure 2B). Thus, the plantaris proteome after repeated CB exposure showed a global pattern that was not identical to that observed after a single CB exposure.

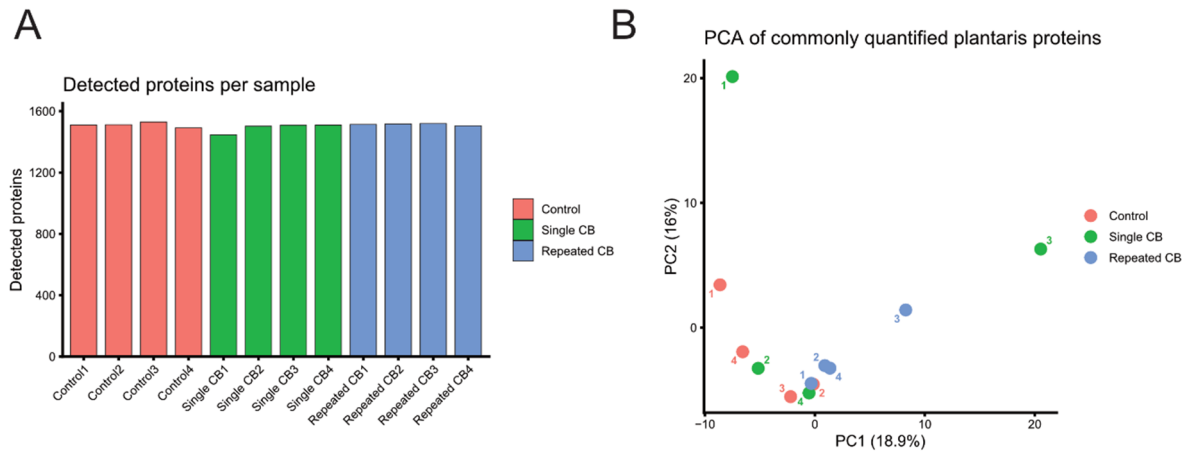


Figure 2. Proteomic overview of plantaris muscle after single and repeated CB exposure. (**A**) Number of detected proteins per sample in plantaris muscles from control, single CB, and repeated CB mice after filtering for Number of Peptides ≥ 2. (**B**) PCA of commonly quantified plantaris proteins after the same filtering. Each point represents one biological sample, and numbers indicate individual sample indices within each group. Data are from n = 4 mice per group.

3.3. Single and Repeated CB Exposure Induced Overlapping but Distinct Proteomic Changes

We next compared protein abundance between groups using the criteria described in Methods. In the single CB versus control comparison, 49 proteins were significantly changed, including 23 increased and 26 decreased proteins (Figure 3A and Supplementary Table S1). In the repeated CB versus control comparison, 74 proteins were significantly changed, including 47 increased and 27 decreased proteins (Figure 3B and Supplementary Table S1). Thus, repeated CB exposure altered a larger number of proteins relative to control than did a single CB exposure.

A direct comparison between repeated CB and single CB muscles identified 32 significantly changed proteins, including 21 increased and 11 decreased proteins in the repeated CB group (Figure 3C and Supplementary Table S1). These results indicate that the single and repeated CB groups exhibited distinct patterns of protein abundance.

We next focused on myosin heavy-chain (MyHC) isoforms, which are major contractile proteins and key determinants of skeletal muscle fiber types. Myh7 (MyHC-I) and Myh2 (MyHC-IIa) abundances were lower in the repeated CB group than in controls, whereas Myh1 (MyHC-IIx) and Myh4 (MyHC-IIb) did not meet the differential-abundance criteria. None of these isoforms met the criteria in the direct comparison between the single and repeated CB groups.

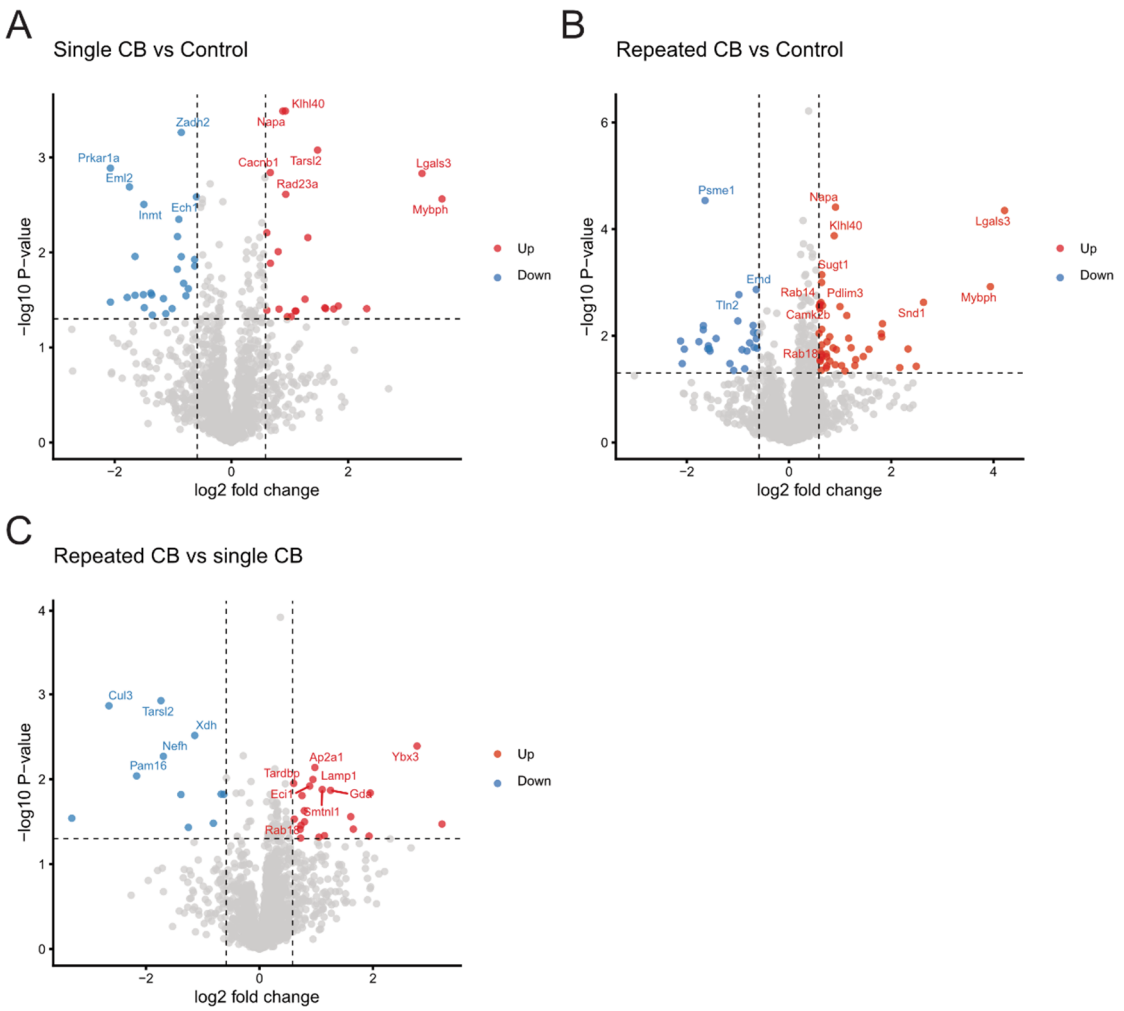


Figure 3. Differential proteomic responses to single and repeated CB exposure. Volcano plots showing differentially changed proteins in plantaris muscle. Comparisons are shown for single CB versus control (**A**), repeated CB versus control (**B**), and repeated CB versus single CB (**C**). Proteins passing the peptide filter described in Methods were analyzed. Red and blue points indicate significantly increased and decreased proteins, respectively, based on $p < 0.05$ and $|\log2 \text{ fold change}| \geq \log2(1.5)$. Differentially changed proteins from each comparison are listed in Supplementary Table S1.

3.4. Functional Enrichment Analysis Identified Biological Categories Associated with Altered Protein Abundance

To characterize the biological functions associated with differentially abundant proteins, we performed Metascape enrichment analysis separately for the three pairwise comparisons. In the single CB versus control comparison, enriched terms included peroxisomal lipid metabolism and regulation of glucose metabolic processes (Supplementary Figure S2A). In the repeated CB versus control comparison, enriched terms included muscle cell proliferation, intracellular protein transport, skeletal muscle cell differentiation, and muscle structure development (Supplementary Figure S2B). In the repeated CB versus single CB comparison, enriched terms included striated muscle contraction, lysosome biogenesis, and endosomal transport (Supplementary Figure S2C).

3.5. Response-Class Analysis Identified Multiple Patterns of CB-Associated Proteomic Remodeling

To characterize protein abundance patterns across the control, single CB, and repeated CB groups, we integrated the three pairwise comparisons and classified differentially abundant proteins into response classes according to the criteria described in Methods (Supplementary Table S2). Among the 130 proteins included in the heatmap, 57 were classified as repeated-specific, 24 as single-versus-repeated difference-only, 13 as sustained, 2 as reinforced, 6 as single-specific/weakly attenuated, 26 as attenuated to baseline, 1 as attenuated, and 1 as reversed (Figure 4 and Supplementary Table S2).

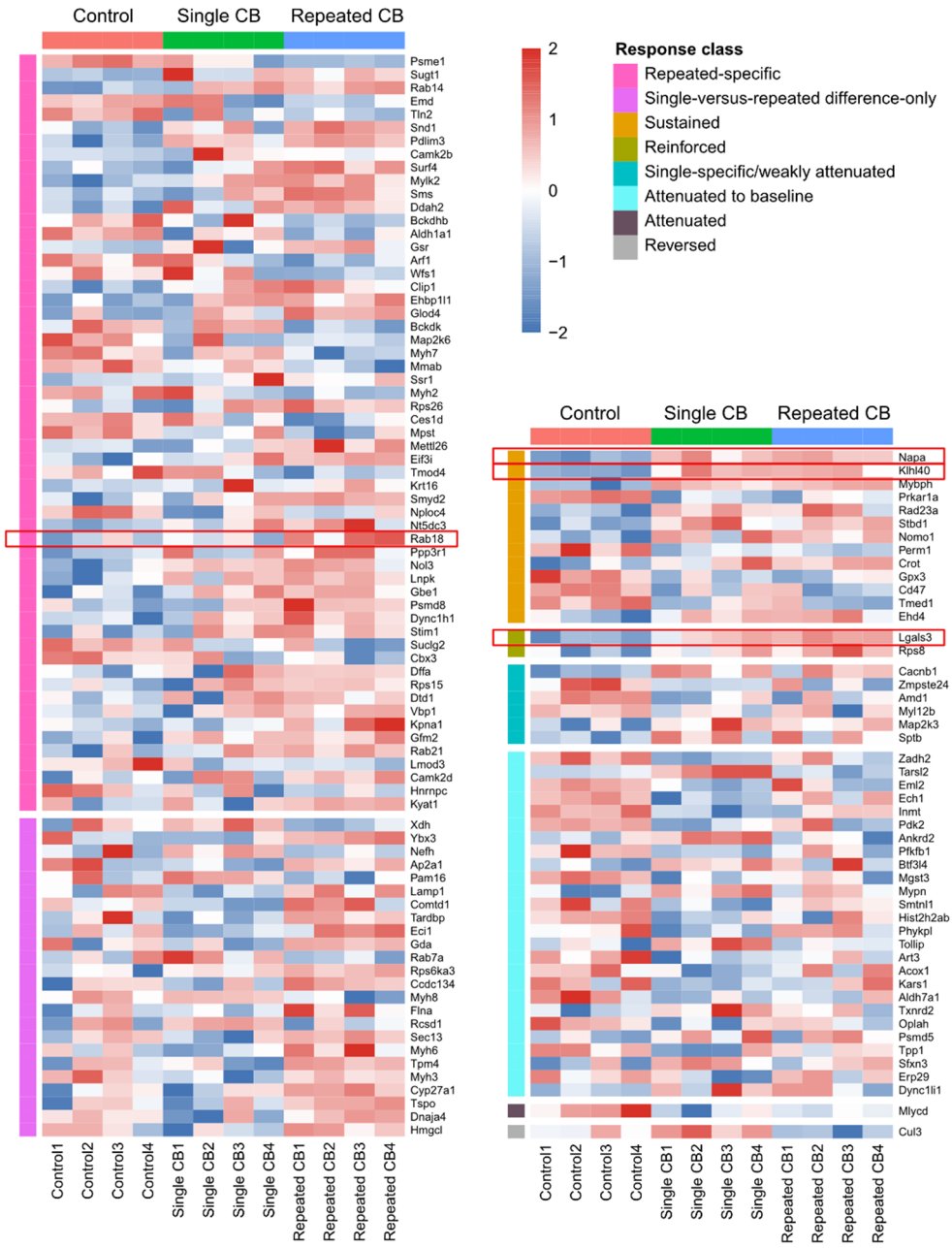


Figure 4. Response-class heatmap of CB-associated proteomic changes. The heatmap shows all 130 response-classified proteins identified by integrated analysis of the three pairwise comparisons, excluding proteins assigned to the unclear-response category. Protein abundance values are shown as row-wise z-scores across control, single CB, and repeated CB samples, with values truncated at −2 and +2 for visualization. Samples are arranged by group, and proteins are grouped according to their response-class assignment. The two heatmap panels group related response classes: repeated-specific and single-versus-repeated difference-only proteins are shown together, whereas sustained, reinforced, single-specific/weakly attenuated, attenuated to baseline, attenuated, and reversed proteins are shown together. Response-class assignments are provided in Supplementary Table S2. Proteins selected for immunoblot validation are highlighted by red boxes.

The heatmap revealed diverse protein abundance patterns across the three groups. The repeated-specific class was the largest, followed by the attenuated-to-baseline and single-versus-repeated difference-only classes. The sustained and reinforced classes included proteins meeting the differential-abundance criteria in both CB-versus-control comparisons, whereas the other classes represented different patterns of protein abundance across the three groups.

Representative proteins in these response classes were associated with diverse biological functions. The sustained class included Klhl40 and Mybph (sarcomere-associated proteins) and Napa (membrane trafficking), whereas the reinforced class included Lgals3/Galectin-3, a tissue-remodeling-related protein. The repeated-specific class included proteins associated with membrane trafficking (Rab14, Rab18, and Rab21), translation

(Rps15 and Rps26), and metabolism (Bckdhb). The attenuated-to-baseline class included metabolic proteins such as Pdk2, Pfkfb1, and Acox1.

3.6. Immunoblotting Validated Selected Response-Class Proteins

Finally, we performed immunoblotting to validate representative proteins from the response classes: Klhl40 and Napa (sustained), Lgals3/Galectin-3 (reinforced), and Rab18 (repeated-specific) (Figure 5A). Immunoblotting showed that Klhl40 was increased in both single CB and repeated CB muscles compared with control muscles, with no significant difference between the two CB groups (Figure 5B). Napa showed a similar pattern, increasing in both CB-treated groups relative to control (Figure 5C). Galectin-3 showed a particularly marked increase after CB exposure and was increased in both single CB and repeated CB muscles (Figure 5D). Rab18 did not significantly differ between control and single CB muscles, but was increased in repeated CB muscles compared with control muscles (Figure 5E). These immunoblotting results confirmed representative proteomic changes identified by the response-class analysis and supported the presence of shared, strongly CB-responsive, and repeated CB-associated protein responses in plantaris muscle.

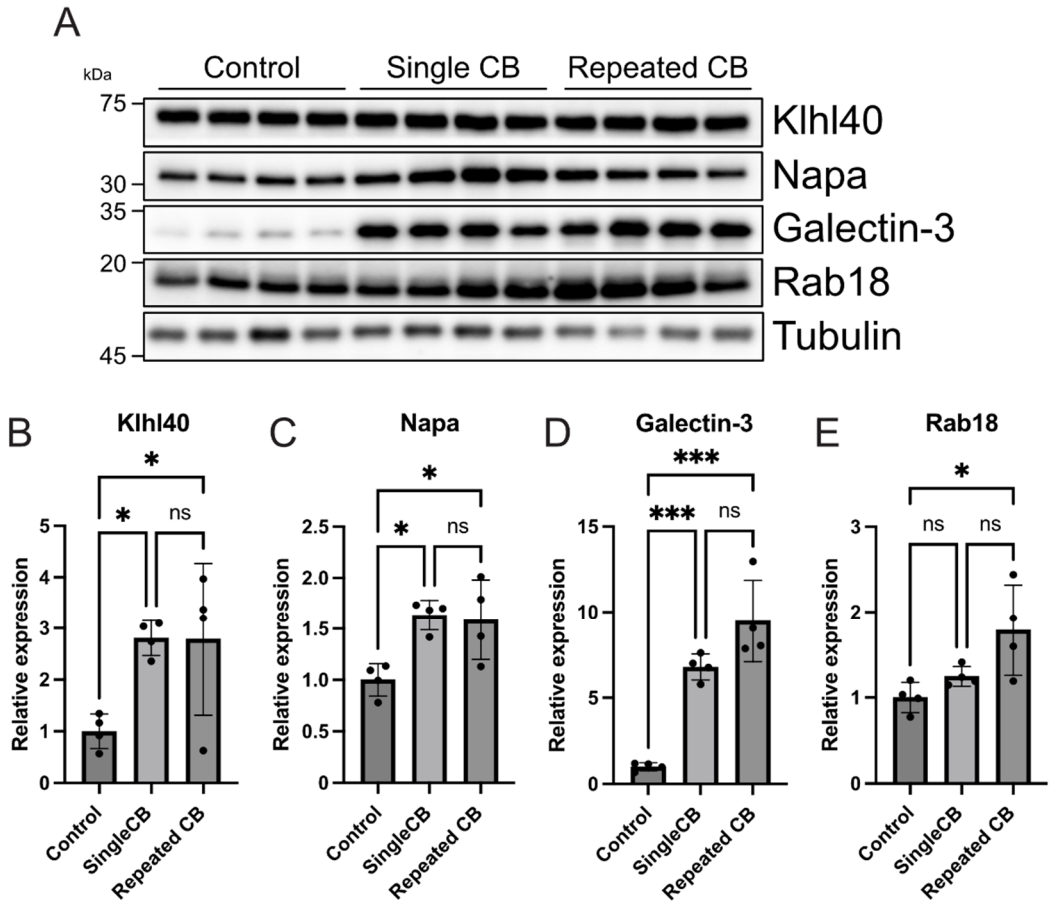


Figure 5. Immunoblot validation of selected response-class proteins. (**A**) Representative immunoblots for Klhl40, Napa, Lgals3/Galectin-3, Rab18, and α-tubulin in plantaris muscles from control, single CB, and repeated CB mice. (**B**–**E**) Quantification of Klhl40 (**B**), Napa (**C**), Lgals3/Galectin-3 (**D**), and Rab18 (**E**) protein abundance. Band intensities were normalized to α-tubulin and expressed relative to the control group. Data are presented as mean ± s.d.; n = 4 mice per group. Data were analyzed by ordinary one-way ANOVA followed by Tukey's multiple-comparison test. ns, not significant; * $p < 0.05$; *** $p < 0.001$. Uncropped immunoblots are provided in Supplementary Figure S3.

4. Discussion

In this study, we established a repeated intermittent CB administration model consisting of 2-week CB treatment periods separated by 4-week washout periods, and examined the effects of single and repeated CB exposure on mouse skeletal muscle using label-free quantitative proteomics. PCA showed that the single CB group

exhibited a relatively dispersed distribution, whereas the repeated CB group formed a more compact cluster. In addition, the sets of significantly altered proteins differed partially among the single CB vs control, repeated CB vs control, and repeated CB vs single CB comparisons. Furthermore, response-class analysis integrating these three pairwise comparisons revealed that the repeated-specific class represented the largest group among clearly classified proteins, indicating that many proteins met the predefined differential-change criteria only in the repeated CB-versus-control comparison. These data demonstrate overlapping but distinct proteomic profiles associated with the single and repeated CB administration regimens.

Recent MS-based proteomic analysis of human skeletal muscle has shown that prolonged β2-adrenergic stimulation with terbutaline increases kelch-like family proteins, including KLHL40 and KLHL41 [17]. In addition, oral CB, but not therapeutic inhaled formoterol, has been reported to increase KLHL41 abundance in human skeletal muscle [24]. In the present study, Klhl40 protein was increased in both the single CB and repeated CB groups. Klhl40 is a skeletal muscle-enriched kelch-like protein, and previous studies have shown that Klhl40 deficiency destabilizes thin filament proteins and causes nemaline-like myopathy, indicating its importance in maintaining sarcomere structure in skeletal muscle [25]. The increase in Klhl40 observed here suggests that CB exposure alters responses related to the contractile apparatus or myofibrillar protein homeostasis in plantaris muscle. Consistent with this interpretation, our proteomic analysis also showed a marked increase in Mybph in both the single CB and repeated CB groups, suggesting that sarcomere-associated proteins are altered after CB exposure. The reduced abundance of Myh7/MyHC-I and Myh2/MyHC-IIa in the repeated CB group further suggests changes in contractile protein composition, although alterations in muscle fiber-type proportions remain unclear. Together, these findings support the possibility that kelch-like family proteins constitute part of a sarcomere-associated proteomic response to prolonged or repeated β2-adrenergic stimulation.

Galectin-3 is a β-galactoside-binding lectin involved in diverse tissue-remodeling processes, including inflammation, immune responses, cell migration, tissue repair, and fibrosis [26,27]. In the present study, Galectin-3 was markedly increased in both CB-treated groups, with no significant difference between the single and repeated CB groups. This result suggests that CB-treated muscle undergoes not only changes in myofiber-associated proteins but also alterations in the tissue environment, including inflammatory, immune, or interstitial remodeling responses. Tissue-wide remodeling involving immune cells, stromal cells, blood vessels, and extracellular matrix components has been reported during muscle hypertrophy [28]. Interestingly, in our proteomic dataset, broad increases in typical extracellular matrix remodeling-related proteins, such as collagen family proteins and Serpinh1, were not clearly observed. Moreover, the present analysis cannot determine whether the increased Galectin-3 was derived from myofibers or from non-myogenic cells such as macrophages or interstitial cells. Therefore, further localization analyses will be required to clarify whether Galectin-3 primarily reflects inflammatory or immune-cell responses, interstitial remodeling, or a myofiber-associated response.

Napa is an alpha-soluble NSF attachment protein (α-SNAP) that functions together with NSF to regulate SNARE complex disassembly and is involved in membrane fusion and vesicular trafficking [29,30]. In this study, Napa was increased in both the single CB and repeated CB groups, indicating that SNARE/NSF-related membrane trafficking proteins are altered after CB exposure in skeletal muscle. Rab18 is a small GTPase implicated in lipid droplets, ER membrane dynamics, and ER–lipid droplet contact sites [31,32]. Rab18 was classified as repeated-specific in the proteomic analysis. Immunoblotting showed increased Rab18 abundance relative to controls in the repeated CB group, although the difference between the two CB-treated groups was not statistically significant. In addition to Rab18, the proteomic analysis identified changes in other membrane trafficking or endomembrane-related proteins, including Rab14, Rab21, Lnpk, and Lamp1. Taken together, the changes in Napa and Rab18 suggest that, in addition to sarcomere-associated and tissue-remodeling-related proteins, proteins involved in membrane fusion, vesicular trafficking, and lipid droplet/ER-associated membrane dynamics are also altered after CB exposure.

A previous human fiber type-specific proteomic study also reported that β2-adrenergic stimulation increases ribosomal proteins and decreases mitochondrial electron transport chain proteins in both type I and type II muscle fibers [33]. In the present study, the repeated CB group showed increased abundance of ribosomal proteins, including Rps15 and Rps26, and decreased abundance of mitochondrial metabolic proteins, including Bckdhb and Suclg2, relative to controls. In the single CB group, metabolic proteins such as Pdk2 and Acox1 were decreased relative to controls. Therefore, although these pathways were not the primary focus of the present analysis, these findings in mouse plantaris muscle partially overlap with proteomic changes reported in human skeletal muscle after β2-adrenergic stimulation.

One limitation of this study is that proteomic measurements were not performed immediately before the final CB treatment period. Therefore, the observed differences between the single and repeated CB groups may reflect both persistent effects of earlier CB exposure and changes occurring during the final treatment period.

5. Conclusions

Single and repeated CB treatment regimens were associated with overlapping but distinct proteomic profiles in mouse plantaris muscle. These differences involved proteins related to sarcomere organization, translation, metabolism, tissue remodeling, and membrane trafficking. These findings provide a foundation for future studies investigating the molecular consequences of different CB administration regimens.

Supplementary Materials

The additional data and information can be downloaded at: https://media.sciltp.com/articles/others/261117091506218 4/PSci-26070249-Supplementary-Materials.zip. Supplementary Figure S1: Muscle-weight changes after 2-week CB treatment and a 4-week post-treatment period; Supplementary Figure S2: Functional enrichment analysis of differentially abundant proteins; Supplementary Figure S3: Uncropped immunoblots for Figure 5; Supplementary Table S1: Differentially changed proteins identified in the three pairwise proteomic comparisons; Supplementary Table S2: Response-class assignments for all 130 proteins displayed in the response-class heatmap.

Author Contributions

Conceptualization, K.H.; methodology, K.H. and H.Y.; investigation, K.H., H.Y., Y.K. and K.T.; formal analysis, K.H. and H.Y.; data curation, K.H. and H.Y.; writing—original draft preparation, K.H.; writing—review and editing, K.H., H.Y., Y.K. and K.T.; supervision, K.H. and K.T.; funding acquisition, K.H. and K.T. All authors have read and agreed to the submitted version of the manuscript.

Funding

Funding was provided in part by JSPS KAKENHI grants 24K22279 and 24K10059; NCNP Intramural Research Grants for Neurological and Psychiatric Disorders, Japan (5–6 and 8–13); and the Japan Sports Agency/MEXT-Japan program for Research and Development on Anti-Doping Science (JADA 2502 and 2602).

Institutional Review Board Statement

Animal procedures were authorized by the Fujita Health University Institutional Animal Care and Use Committee, Japan (approval No. APU25120-MD1), and were performed under the relevant institutional animal-care rules.

Informed Consent Statement

Not applicable.

Data Availability and Statistical Reporting

Values are shown as mean ± s.d. GraphPad Prism 9 was used for statistical analyses of body weight, muscle weight, and immunoblot quantification. In Figure 1, body weight and muscle-weight data from the repeated intermittent CB experiment were evaluated by ordinary one-way ANOVA followed by Tukey's multiple-comparison test. In Supplementary Figure S1, data from the 2-week treatment and 4-week post-treatment experiment were analyzed by ordinary two-way ANOVA using treatment and time point as factors, followed by Šídák's multiple-comparison test for control-versus-CB comparisons within each time point. Immunoblot quantification across the control, single CB, and repeated CB groups was analyzed by ordinary one-way ANOVA followed by Tukey's multiple-comparison test. For these analyses, statistical significance was set at $p < 0.05$. For the proteomic analyses, pairwise differences in protein abundance were evaluated using Student's *t*-tests in Perseus. Proteins were considered differentially changed based on a nominal p value < 0.05, $|\log2 \text{ fold change}| \geq \log2(1.5)$, and Number of Peptides ≥ 2. No multiple-testing correction was applied to the primary differential-change criteria. The figure legends specify the sample sizes and statistical tests used for each dataset. Supplementary Table S1 contains the proteins identified as differentially changed in the three pairwise proteomic comparisons. Supplementary Table S2 provides the response-class assignments for all 130 proteins included in the response-class heatmap. Supplementary Figure S3 contains the uncropped immunoblot images. The LC-MS/MS raw files generated in this study have been deposited in the ProteomeXchange Consortium [34] via jPOST [35]

under the dataset identifiers PXD080839 and JPST004754. Other data supporting the conclusions of this study are available from the corresponding author upon reasonable request.

Acknowledgments

We gratefully acknowledge E. Fukushima, S. Takeuchi, C. Ohshima, and the staff of Fujita Health University Open Facility Center for experimental assistance.

Conflicts of Interest

The authors declare no conflict of interest.

Use of AI and AI-Assisted Technologies

ChatGPT (OpenAI) was used only for English editing and organization of the manuscript text. All scientific content, data presentation, and interpretation were checked and finalized by the authors.

References

1. Lynch, G.S.; Ryall, J.G. Role of β-Adrenoceptor Signaling in Skeletal Muscle: Implications for Muscle Wasting and Disease. *Physiol. Rev.* **2008**, *88*, 729–767. https://doi.org/10.1152/physrev.00028.2007.
2. Hostrup, M.; Onslev, J. The Beta2-adrenergic Receptor—A Re-emerging Target to Combat Obesity and Induce Leanness? *J. Physiol.* **2022**, *600*, 1209–1227. https://doi.org/10.1113/jp281819.
3. Reeds, P.J.; Hay, S.M.; Dorward, P.M.; et al. The Effect of β-Agonists and Antagonists on Muscle Growth and Body Composition of Young Rats (Rattus Sp.). *Comp. Biochem. Physiol. Part C: Comp. Pharmacol.* **1988**, *89*, 337–341. https://doi.org/10.1016/0742-8413(88)90234-4.
4. Hinkle, R.T.; Hodge, K.M.B.; Cody, D.B.; et al. Skeletal Muscle Hypertrophy and Anti-atrophy Effects of Clenbuterol Are Mediated by the β2-adrenergic Receptor. *Muscle Nerve* **2002**, *25*, 729–734. https://doi.org/10.1002/mus.10092.
5. Ryall, J.G.; Sillence, M.N.; Lynch, G.S. Systemic Administration of β2-adrenoceptor Agonists, Formoterol and Salmeterol, Elicit Skeletal Muscle Hypertrophy in Rats at Micromolar Doses. *Br. J. Pharmacol.* **2006**, *147*, 587–595. https://doi.org/10.1038/sj.bjp.0706669.
6. Meister, J.; Bone, D.B.J.; Knudsen, J.R.; et al. Clenbuterol Exerts Antidiabetic Activity through Metabolic Reprogramming of Skeletal Muscle Cells. *Nat. Commun.* **2022**, *13*, 22. https://doi.org/10.1038/s41467-021-27540-w.
7. Kim, J.; Grotegut, C.A.; Wisler, J.W.; et al. β-Arrestin 1 Regulates β2-Adrenergic Receptor-Mediated Skeletal Muscle Hypertrophy and Contractility. *Skelet. Muscle* **2018**, *8*, 39. https://doi.org/10.1186/s13395-018-0184-8.
8. Burniston, J.G.; Clark, W.A.; Tan, L.; et al. Dose-dependent Separation of the Hypertrophic and Myotoxic Effects of the β2-adrenergic Receptor Agonist Clenbuterol in Rat Striated Muscles. *Muscle Nerve* **2006**, *33*, 655–663. https://doi.org/10.1002/mus.20504.
9. Rothwell, N.J.; Stock, M.J.; Sudera, D.K. Changes in Tissue Blood Flow and β-receptor Density of Skeletal Muscle in Rats Treated with the β2-adrenoceptor Agonist Clenbuterol. *Br. J. Pharmacol.* **1987**, *90*, 601–607. https://doi.org/10.1111/j.1476-5381.1987.tb11211.x.
10. Sato, S.; Nomura, S.; Kawano, F.; et al. Adaptive Effects of the β2-Agonist Clenbuterol on Expression of β2-Adrenoceptor mRNA in Rat Fast-Twitch Fiber-Rich Muscles. *J. Physiol. Sci.* **2010**, *60*, 119–127. https://doi.org/10.1007/s12576-009-0075-1.
11. Guddat, S.; Fußhöller, G.; Geyer, H.; et al. Clenbuterol—Regional Food Contamination a Possible Source for Inadvertent Doping in Sports. *Drug Test. Anal.* **2012**, *4*, 534–538. https://doi.org/10.1002/dta.1330.
12. Thevis, M.; Geyer, L.; Geyer, H.; et al. Adverse Analytical Findings with Clenbuterol among U-17 Soccer Players Attributed to Food Contamination Issues. *Drug Test. Anal.* **2013**, *5*, 372–376. https://doi.org/10.1002/dta.1471.
13. Parr, M.K.; Blokland, M.H.; Liebetrau, F.; et al. Distinction of Clenbuterol Intake from Drug or Contaminated Food of Animal Origin in a Controlled Administration Trial—The Potential of Enantiomeric Separation for Doping Control Analysis. *Food Addit. Contam.: Part A* **2017**, *34*, 525–535. https://doi.org/10.1080/19440049.2016.1242169.
14. Spiller, H.A.; James, K.J.; Scholzen, S.; et al. A Descriptive Study of Adverse Events from Clenbuterol Misuse and Abuse for Weight Loss and Bodybuilding. *Subst. Abus.* **2013**, *34*, 306–312. https://doi.org/10.1080/08897077.2013.772083.
15. Grimmer, N.M.; Gimbar, R.P.; Bursua, A.; et al. Rhabdomyolysis Secondary to Clenbuterol Use and Exercise. *J. Emerg. Med.* **2016**, *50*, e71–e74. https://doi.org/10.1016/j.jemermed.2015.09.006.
16. Burniston, J.G.; McLean, L.; Beynon, R.J.; et al. Anabolic Effects of a Non-myotoxic Dose of the β2-adrenergic Receptor Agonist Clenbuterol on Rat Plantaris Muscle. *Muscle Nerve* **2007**, *35*, 217–223. https://doi.org/10.1002/mus.20684.

17. Jessen, S.; Prats Quesada, J.; Di Credico, A.; et al. Beta2-Adrenergic Stimulation Induces Resistance Training-Like Adaptations in Human Skeletal Muscle: Potential Role of KLHL41. *Scand. J. Med. Sci. Sports* **2024**, *34*, e14736. https://doi.org/10.1111/sms.14736.
18. Kim, K.H.; Kim, Y.S.; Yang, J. The Muscle-hypertrophic Effect of Clenbuterol Is Additive to the Hypertrophic Effect of Myostatin Suppression. *Muscle Nerve* **2011**, *43*, 700–707. https://doi.org/10.1002/mus.21950.
19. Hitachi, K.; Yamaguchi, H.; Tsuchida, K. Proteomic Analysis Data of Skeletal Muscle Tissue in Myosin Heavy Chain -IIx and -IIb Double Knockout Mice. *J. Proteome Data Methods* **2025**, *7*, 2. https://doi.org/10.14889/jpdm.2025.0002.
20. Hitachi, K.; Kiyofuji, Y.; Yamaguchi, H.; et al. Simultaneous Loss of Skeletal Muscle Myosin Heavy Chain IIx and IIb Causes Severe Skeletal Muscle Hypoplasia in Postnatal Mice. *FASEB J.* **2023**, *37*, e22692. https://doi.org/10.1096/fj.202200581r.
21. Hughes, C.S.; Moggridge, S.; Müller, T.; et al. Single-Pot, Solid-Phase-Enhanced Sample Preparation for Proteomics Experiments. *Nat. Protoc.* **2019**, *14*, 68–85. https://doi.org/10.1038/s41596-018-0082-x.
22. Tyanova, S.; Temu, T.; Sinitcyn, P.; et al. The Perseus Computational Platform for Comprehensive Analysis of (Prote)Omics Data. *Nat. Methods* **2016**, *13*, 731–740. https://doi.org/10.1038/nmeth.3901.
23. Zhou, Y.; Zhou, B.; Pache, L.; et al. Metascape Provides a Biologist-Oriented Resource for the Analysis of Systems-Level Datasets. Nat. Commun. **2019**, 10, 1523. https://doi.org/10.1038/s41467-019-09234-6.
24. Hostrup, M.; Moesgaard, L.; Thomassen, M.; et al. Clenbuterol, but Not Inhaled Formoterol, Upregulates the Sarcomere Stabilizer KLHL41 to a Similar Extent as Resistance Training in Human Skeletal Muscle. *Drug Test. Anal.* **2026**, *18*, 66–73. https://doi.org/10.1002/dta.3963.
25. Garg, A.; O'Rourke, J.; Long, C.; et al. KLHL40 Deficiency Destabilizes Thin Filament Proteins and Promotes Nemaline Myopathy. *J. Clin. Investig.* **2014**, *124*, 3529–3539. https://doi.org/10.1172/jci74994.
26. Johannes, L.; Jacob, R.; Leffler, H. Galectins at a Glance. *J. Cell Sci.* **2018**, *131*, jcs208884. https://doi.org/10.1242/jcs.208884.
27. Cerri, D.G.; Rodrigues, L.C.; Alves, V.M.; et al. Endogenous Galectin-3 Is Required for Skeletal Muscle Repair. *Glycobiology* **2021**, *31*, 1295–1307. https://doi.org/10.1093/glycob/cwab071.
28. Brightwell, C.R.; Latham, C.M.; Thomas, N.T.; et al. A Glitch in the Matrix: The Pivotal Role for Extracellular Matrix Remodeling during Muscle Hypertrophy. *Am. J. Physiol.-Cell Physiol.* **2022**, *323*, C763–C771. https://doi.org/10.1152/ajpcell.00200.2022.
29. Hay, J.C.; Scheller, R.H. SNAREs and NSF in Targeted Membrane Fusion. *Curr. Opin. Cell Biol.* **1997**, *9*, 505–512. https://doi.org/10.1016/s0955-0674(97)80026-9.
30. Ryu, J.-K.; Min, D.; Rah, S.-H.; et al. Spring-Loaded Unraveling of a Single SNARE Complex by NSF in One Round of ATP Turnover. *Science* **2015**, *347*, 1485–1489. https://doi.org/10.1126/science.aaa5267.
31. Ozeki, S.; Cheng, J.; Tauchi-Sato, K.; et al. Rab18 Localizes to Lipid Droplets and Induces Their Close Apposition to the Endoplasmic Reticulum-Derived Membrane. *J. Cell Sci.* **2005**, *118*, 2601–2611. https://doi.org/10.1242/jcs.02401.
32. Xu, D.; Li, Y.; Wu, L.; et al. Rab18 Promotes Lipid Droplet (LD) Growth by Tethering the ER to LDs through SNARE and NRZ Interactions. *J. Cell Biol.* **2018**, *217*, 975–995. https://doi.org/10.1083/jcb.201704184.
33. Jessen, S.; Di Credico, A.; Moreno-Justicia, R.; et al. Fibre Type–Specific Proteomics Reveals Shared and Distinct Skeletal Muscle Adaptations to Resistance Training and Beta2-Adrenergic Agonist. *J. Cachexia, Sarcopenia Muscle* **2026**, *17*, e70175. https://doi.org/10.1002/jcsm.70175.
34. Deutsch, E.W.; Csordas, A.; Sun, Z.; et al. The ProteomeXchange Consortium in 2017: Supporting the Cultural Change in Proteomics Public Data Deposition. *Nucleic Acids Res.* **2017**, *45*, D1100–D1106. https://doi.org/10.1093/nar/gkw936.
35. Okuda, S.; Watanabe, Y.; Moriya, Y.; Kawano, S.; Yamamoto, T.; Matsumoto, M.; Takami, T.; Kobayashi, D.; Araki, N.; Yoshizawa, A.C.; et al. jPOSTrepo: An International Standard Data Repository for Proteomes. *Nucleic Acids Res.* **2017**, *45*, D1107–D1111. https://doi.org/10.1093/nar/gkw1080.